Dyes and Pigments 139 (2017) 193–200

Contents lists available at ScienceDirect

Dyes and Pigments

journal homepage: www.elsevier.com/locate/dyepig

Aerogels containing 5,10,15,20-tetrakis-(4-sulfonatophenyl)-porphyrin with controlled state of aggregation

Juan Pablo Pino-Pinto [a], Felipe Oyarzun-Ampuero [b], Sandra L. Orellana [a], Mario E. Flores [a], Hiroyuki Nishide [c], Ignacio Moreno-Villoslada [a, *]

[a] Instituto de Ciencias Químicas, Facultad de Ciencias, Universidad Austral de Chile, Casilla 567, Valdivia, Chile
[b] Departamento de Ciencias y Tecnología Farmaceúticas, Facultad de Ciencias Químicas y Farmacéuticas, Universidad de Chile, Santos Dumont 964, Santiago 8380494, Chile
[c] Department of Applied Chemistry, School of Science and Engineering, Waseda University, Tokyo 169-8555, Japan

ARTICLE INFO

Article history:
Received 25 August 2016
Received in revised form
23 November 2016
Accepted 5 December 2016
Available online 8 December 2016

Keywords:
Aromatic-aromatic interactions
Dye aggregation
Dye in solid materials
Porphyrins
Aromatic polycations

ABSTRACT

Aerogels made of chitosan and chondroitin sulfate, and containing 5,10,15,20-tetrakis-(4-sulfonatophenyl)-porphyrin have been synthesized. The aerogels presented a microstructure made of microfibers and microsheets, with porosity higher than 99%. The dispersion and state of aggregation of the dye in the solids have been controlled with the aid of aromatic polyelectrolytes able to produce aromatic-aromatic interactions. Thus, non-homogenous dispersions of the dye as J-aggregates and formation of microcrystals on the microsheet surface were observed in the absence of the aromatic polymers; on the contrary, well dispersed H-aggregates of the dye were observed in the presence of poly(decylviologen), and well dispersed complexed monomeric dye molecules were found in the presence of a polyketone derivatized with hystamine, thus presenting imidazolium pendant groups. The same state of aggregation has been observed in solution for the respective complexes, highlighting the potential of aromatic-aromatic interactions to achieve a control of the state of aggregation of dyes in solution and further transfer to the solid state keeping their photophysical properties, and furnishing means for a good dispersion of the dyes in solid materials.

1. Introduction

The formation of materials in which dyes are homogenously dispersed is of interest, not only for the good staining and aesthetical characteristics, but also for the functional performance of such materials. In addition, the state of aggregation of dyes may determine both the homogeneity of their dispersion in materials and their functionality. Aggregation may be avoided to enhance light harvesting and energy transfer in dye applications such as electron transfer in electronic devices [1], or photosensitizing in photodynamic therapy (PDT) [2]. However, well defined and controlled aggregate structures of dyes may enhance the global energy-conversion efficiencies of organic dye-sensitized solar cells and photocatalysts [3,4]. Porphyrins are efficient photosensitizers for PDT against cancer [5]. The therapy is based on the energy transfer from an excited state of the photosensitizer to oxygen upon irradiation, generating singlet oxygen which produces cell damage in tumor tissues [6–8]. The action of a photosensitizer is influenced by the environmental conditions concerning both thermodynamic and kinetic properties. The self-aggregation state, distribution, interactions, and reactivity with surrounding molecules may determine the life-time of excited states and the overall ability to produce singlet oxygen [2]. This highlights the need of achieving a good control of the dispersion and aggregation state of dyes such as porphyrins in functional solid materials for technological applications such as PDT.

It is well known the tendency of water-soluble aromatic dyes to form self-aggregates at increasing concentration, stabilized by dispersion forces [9–23]. Higher order aggregates of charged dyes can be found on complementary charged surfaces, since charge compensation minimizes charge repulsion, producing a higher local concentration of dyes and consequent aggregation, frequently undergoing cooperative binding [24]. Disaggregation of dyes can be achieved by the use of amphiphilic species such as surfactants or amphiphilic polymers [9,13,25]. A good control of assembled

* Corresponding author.
E-mail address: imorenovilloslada@uach.cl (I. Moreno-Villoslada).

http://dx.doi.org/10.1016/j.dyepig.2016.12.005
0143-7208/

structures, such as nanostructures between dendrimers and dyes [26–29], has been achieved by electrostatic self-assembly [26–33]. In order to control and modulate the state of aggregation of dyes when interacting with substrates, apart from primary long-range electrostatic interactions and dispersion forces, secondary interactions such as hydrogen bonding or aromatic-aromatic interactions may play a crucial role [12,34–36]. In this sense, the use of polyelectrolytes able to produce secondary interactions with complementary charged dyes may constitute a means of controlling the state of aggregation and dispersion efficiency of dyes. Investigations concerning the interactions of dyes and polymers in solution have shown that polyelectrolytes presenting charged aromatic groups are able to modulate the state of aggregation of dyes, since aromatic-aromatic interactions between the dye and the aromatic groups of the polymer may be stronger than dye-to-dye interactions [20,22,37,38]. The physicochemical characteristics of the polymers are also important, such as their linear aromatic density, amphiphilia, and flexibility. Thus, we have demonstrated that polymers such as poly(4-vinylpyridine), polyketone derivatives with pendant pyridinium and imidazolium groups, poly(vinylpyrrolidones)s modified with aromatic amines, or poly(viologen)s are able to modify the transition pH between the tetra-anionic form of 5,10,15,20-tetrakis-(4-sulfonatophenyl)-porphyrin (TPPS) and its di-anionic form, as well as its state of aggregation, as compared to the behavior of the pristine dye [12,13,39].

Chitosan (CS)/chondroitin sulfate (ChS) aerogels are ultralight, porous solid materials designed to induce wound healing in chronic wounds such as diabetic foot and venous ulcers. They are non-toxic, biocompatible and biodegradable materials. Interestingly, some of their effects in tissues are based on strong angiogenic properties [40]. They are synthesized by freeze-drying aqueous colloidal suspensions of polysaccharide nanocomplexes. The mechanical properties of these materials facilitate their application in open wounds, easily adapting to the wound contour due to their low toughness and hydration ability. In addition to their physiological activity, they may also serve as carriers of active molecules, such as photosensitizers for PDT, which may promote the new materials for novel applications.

In this paper, we will study the incorporation of TPPS in CS/ChS aerogels in terms of homogeneity of dispersion and control of its state of aggregation by means of the use of aromatic polyelectrolytes. Thus, we will answer the question whether the dye aggregation and photophysical effects observed in solution concerning the TPPS/aromatic polycation complexes can be transferred to solid materials composed of charged polysaccharides, dyes, and aromatic excipients, fabricated form stable colloidal suspensions which are further subjected to an out-of-equilibrium process such as freeze-drying.

2. Experimental

2.1. Materials

TPPS (TCI) was used without further purification. CS (Protasan™ UP CL 213, Novamatrix, 83% deacetylation, molecular mass of

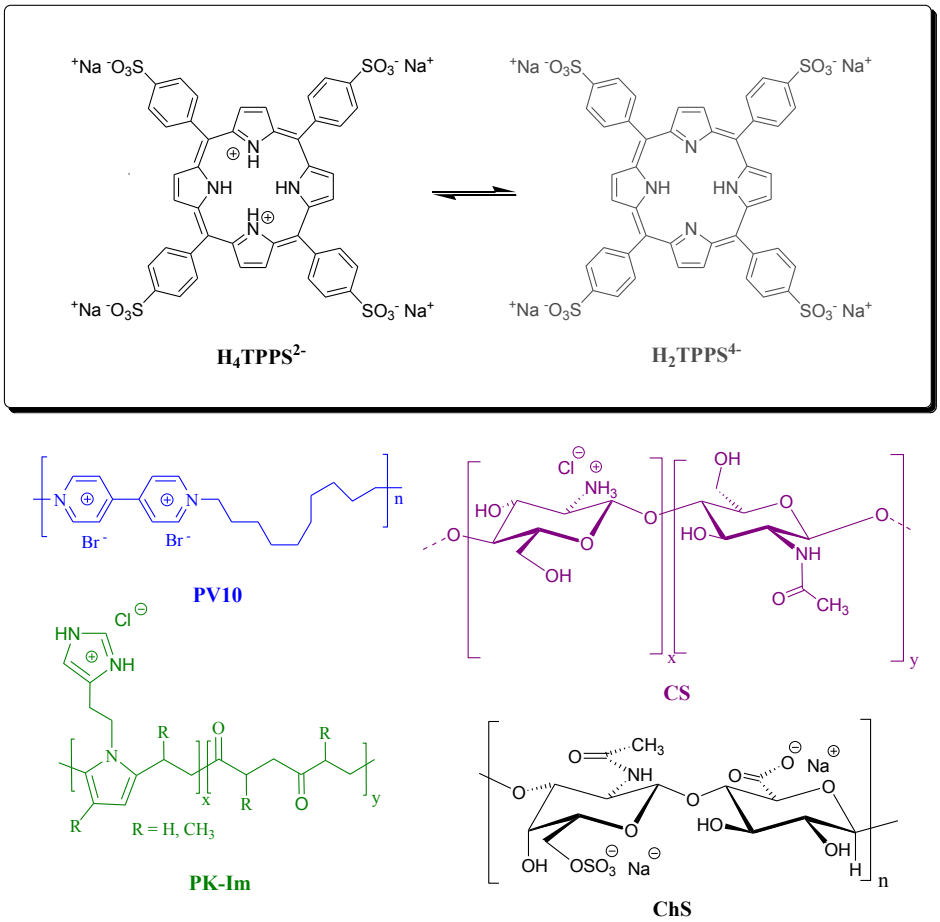

Fig. 1. Molecular structures of the di-anionic and tetra-anionic forms of TPPS and the polymers used.

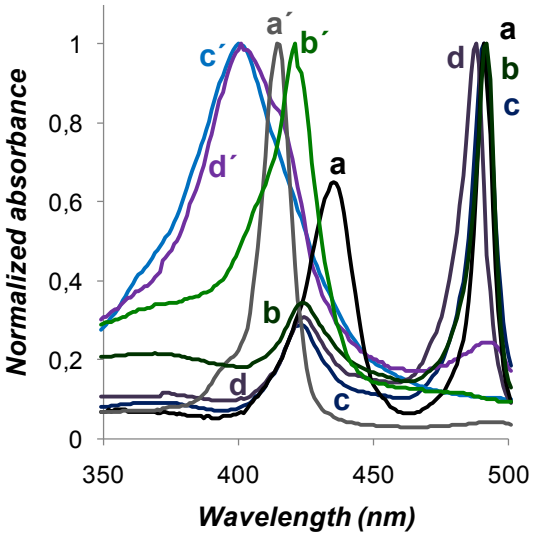

Fig. 2. Normalized UV–vis spectra of 10^{-5} M of TPPS at pH 1 (a–d) and around 6 (á–d́) in the absence of any polyelectrolyte (a, a´), and in the presence of 10^{-3} M of PK-Im (b, b´), PV10 (c, c´), and CS (d, d´).

239.22 g/mol of amino units considered) and ChS (chondroitin sulfate A sodium salt from bovine trachea, Sigma-Aldrich, molecular mass of 252 g/mol of ionizable groups considered), have been used to prepare the aerogels. A polyketone derivative containing pendant imidazolium groups (PK-Im, molecular mass of 266 g/mol of basic groups considered), and poly(decylviologen) (PV10, molecular mass of 456 g/mol of bipyridinium residues considered) were used to control the dispersion and state of aggregation of the dye. The synthesis of PK-Im [12], and PV10 [39] has been reported elsewhere. Deionized water was used as solvent. The pH was adjusted with minimum amounts of HCl (Fisher Scientific) and NaOH (Merck). The structures of the polymers and TPPS in both its basic and acid forms are shown in Fig. 1.

2.2. Equipment

Distilled water was deionized in a Simplicity Millipore deionizer.

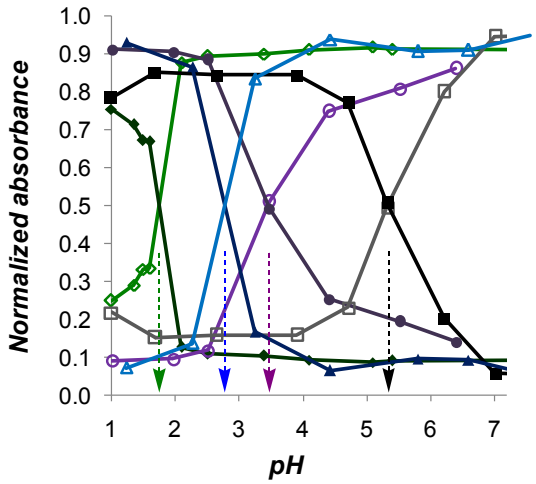

Fig. 3. Transition pH between H_4TPPS^{2-} and H_2TPPS^{4-} at a concentration of 10^{-5} M in the absence of any polyelectrolyte (■, □), and in the presence of 10^{-3} M of PK-Im (◆, ◇), PV10 (▲, △), and CS (●, ○).

The pH was controlled on an UltraBasic Denver Instrument pH meter. UV–vis measurements were performed in a Helios γ spectrophotometer. Fluorescence was analyzed in a SCINCO FluoroMate FS-2 spectrometer. The colloidal suspensions were prepared with the aid of a NE-1600/NE-1800 New Era Pump Systems perfusion pump. Apparent size and zeta potential of suspended nanoparticles were obtained by dynamic light scattering (DLS) and laser Doppler anemometry on a Malvern Zetasizer Nano ZS (Malvern) instrument with backscatter detection (173°), controlled by the Dispersion Technology Software (DTS 6.2, Malvern). Freeze-drying of colloidal suspensions was carried out in an Alpha 1–2 LD plus lyophilizer (Christ). Optical microscopy of the resulting materials was done in an Axiovert 40 CFL Carl Zeiss microscope. In addition, confocal fluorescence microscopy of the solid materials was performed in a FluoView 1000 Olympus microscope. Diffuse reflectance UV–vis spectroscopy was performed in a Perkin Elmer Lambda 35 spectrophotometer, equipped with a LabSphere RSA-PE-20 integrating sphere, and controlled by the WinLab version 2.85 software. A Spectralon standard (LabSphere) was used as blank. Fluorescence studies of the aerogels containing TPPS were done in a PerkinElmer LS 55 fluorescence spectrometer, equipped with a Front Surface accessory to measure solid samples.

2.3. Procedures

Formulations and analyses were done following conventional procedures. Particular experimental conditions are provided in the captions of Figs. 2–4 and 8. *Interaction studies*. Aqueous solutions of polymers and TPPS were prepared, and absorption and emission UV–vis analyses were performed using quartz vessels with path lengths of 1 cm. All samples were prepared in pure water and allowed equilibrating after pH adjustment for several minutes. *Collodial suspensions*. Colloidal suspensions were obtained by simultaneously adding dropwise (using 20 mL plastic syringes and a perfusion pump) stock solutions of CS and ChS (4 mL of each solution at concentration of 10^{-2} M, and pH 4.3 ± 0.2 for CS and 5.0 ± 0.2 for ChS) at a flux of 880 μL min^{-1} into a 50 mL flask of 36 mm of diameter containing 10 mL of deionized water or an aqueous solution of the complex TPPS/aromatic polycation, at 15 °C and pH 5.0, and gently stirring with a magnetic stirrer. The final pH obtained was 4.7. In order to prepare colloidal suspensions comprising CS, ChS, and TPPS, without incorporating any aromatic polycation, the dye was dissolved together with ChS and placed in the same syringe. The colloidal suspensions were characterized by analysis of apparent particle size, polydispersity index (PDI), and zeta potential as a function of time. *Aerogel formation and characterization*. After the colloidal suspensions were formed, the total volume (18 mL) was frozen in the same container at −15 °C for 24 h, and then freeze-dried at 0.050 mbar and condenser temperature of −57 °C for 72 h. If necessary, the resulting aerogels were stored at 4 °C in closed containers containing dried silica gel, in order to avoid moisture. The aerogels were characterized by optical microscopy and absorption and emission UV–vis spectroscopy. Data for UV–vis absorption spectroscopy of solids was acquired as relative reflectance (R), and subsequently transformed with the Kubelka-Munk equation, which correlates the diffuse reflectance with absorption, according to $(1 - R)^2/2R = K/S$, where K and S are the molar absorption and the scattering coefficients, respectively.

3. Results and discussion

3.1. TPPS interaction with polycations in solution

The polycations used in this study present different characteristics towards the interaction with TPPS. All the polymers stabilize

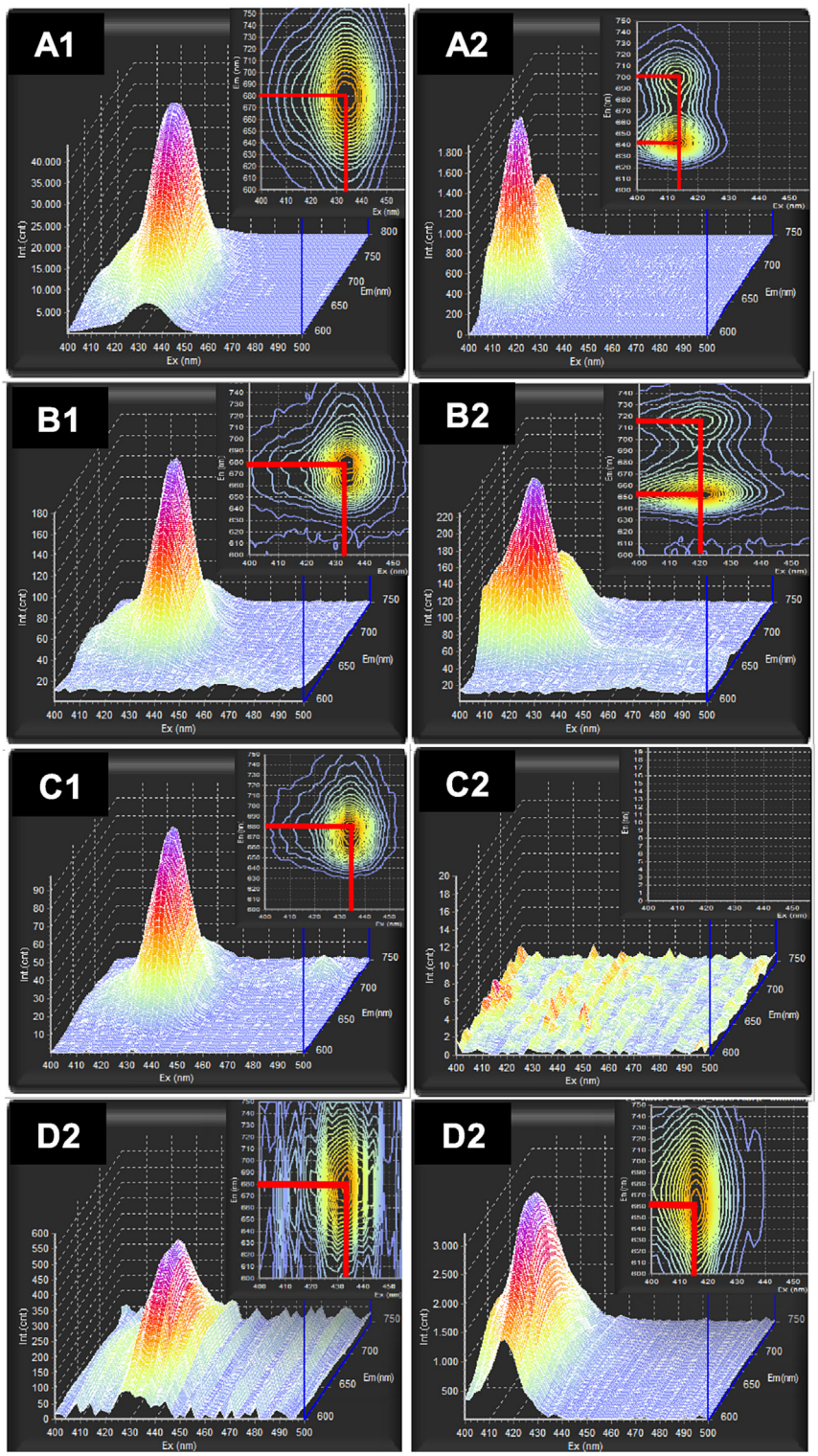

Fig. 4. Three dimensional fluorescence graphs showing fluorescence intensity as a function of excitation and emission wavelengths of 10^{-6} M of TPPS at pH around 1 (entries X1) and >5 (entries X2), in the absence of any polymer (entries A1 and A2), and in the presence of 10^{-4} M of PK-Im (B1 and B2), PV10 (C1 and C2), and CS (D1 and D2).

J-aggregates of the di-anionic H_4TPPS^{2-} at very low pH, revealed by the appearance of a band at around 500 nm, as can be seen in Fig. 2. However, at pH around 6, the three polymers induce different aggregation patterns. pK-Im stabilizes the monomeric form of H_2TPPS^{4-}, and the corresponding monomer band appears at 424 nm, indicating the close contact between the polymer and the dye, as a consequence of which water from the hydration sphere of the dye is released, producing the absorbance band shift to lower energies [10–12]. Aromatic-aromatic interactions between the imidazolium groups and the porphyrin, and the polymer amphiphilia, allows the dispersion of the dye molecules in the polymer domain. On the contrary, PV10 induces H-aggregates revealed by a

well-formed band centered at around 400 nm. The high flexibility of this polymer is invoked in order to explain the stability of these aggregates, which may be wrapped by the polymer [12,39]. CS does also produce H-aggregates, as can be seen in Fig. 2, line d. Interestingly, additional bands centered at 414 nm, corresponding to the hydrated monomeric H_2TPPS^{4-}, and at around 500 nm, corresponding to J-aggregates of the di-anionic H_4TPPS^{2-}, are observed, indicating the co-existence of the dye at different states of aggregation and protonation. These results can be specifically related to the polysaccharide nature of CS, which present a rigid geometry, tending to an expanded helical conformation in which each glucosamine unit is turned a certain degree with respect to the adjacent one with the amino groups of alternating monomeric units pointing to opposite directions with respect to the molecular axis, and presenting a low linear charge density [41]. Attractive interactions make dye molecules concentrate around the polymer chains producing mainly H-aggregates or tetra-anionic monomers at basic and moderate acid pH, and J-aggregates of di-anionic species at strong acid pH. All these states of aggregation co-exist depending on the pH, proving the stepwise protonation/deprotonation of the polymer-bound dye [42]. Due to its polymeric nature, deprotonation of the polysaccharide also occurs stepwise, so that, upon increasing the pH, the linear charge density continuously decreases, and the dye progressively undergoes weaker interaction forces with the polymer, and disperses in its monomeric tetra-anionic form. While increasing the pH from 2 to 7, the H- and monomer bands of the tetra-anionic species centered at around 400 and 414 nm, respectively, continuously grows at the expense of the J-band, and from pH 4.5 the monomer band of the tetra-anionic species grows at the expense of the corresponding H-band so that at pH over 7 only the monomer band at 414 nm appears (data not shown). In addition, chiral configurations of these aggregates are observed, as deduced by the strong Cotton effect observed in circular dichroism experiments [42]. The special polymer geometry may cause, in addition, that the J-band of H_4TPPS^{2-} at low pHs is shifted to higher energies with respect to that in the absence or in the presence of the other polymers, indicating a different conformation of the head-to-tail stacked aggregates.

In addition, all the polycations produce a different shift of the transition pH between the tetra-anionic form of the dye (H_2TPPS^{4-}) and the di-anionic species (H_4TPPS^{2-}). Thus, the transition pH found in solutions of 10^{-5} M of TPPS is 5.2 for the pristine dye,

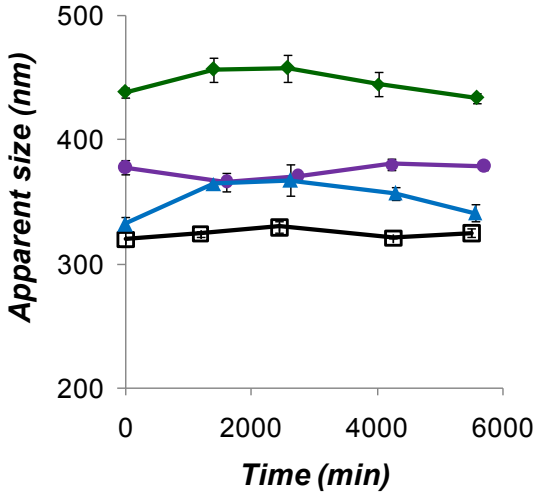

Fig. 5. Apparent size of nanoparticles in colloidal suspensions of CS/ChS (□), CS/TPPS/ChS (●), CS/TPPS/PK-Im/ChS (◆), and CS/TPPS/PV10/ChS (▲), as a function of time.

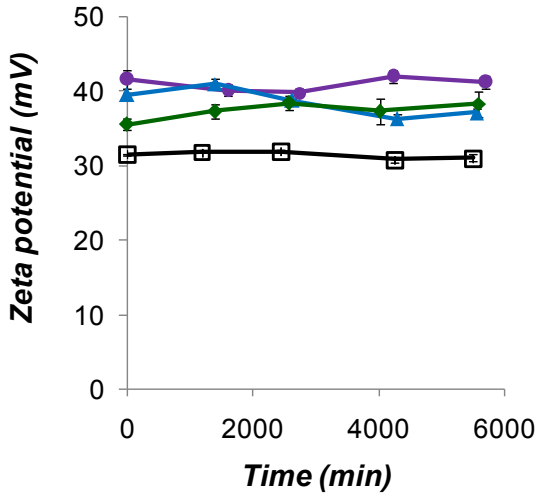

Fig. 6. Zeta potential of nanoparticles in colloidal suspensions of CS/ChS (□), CS/TPPS/ChS (●), CS/TPPS/PK-Im/ChS (◆), and CS/TPPS/PV10/ChS (▲), as a function of time.

while in the presence of 100-fold, PK-Im, PV10, and CS is 1.8, 2.8, and 3.4, respectively, as can be seen in Fig. 3, where for each system the absorbance intensity of the bands corresponding to the di-anionic and tetra-anionic species of the dye has been plotted normalized for their sum at every pH. This change on the transition pH may be explained according to different interpretations. If pure long-range electrostatic interactions are held, the negative charge of the hydrated dyes is stabilized by the positive charge of the polymers. In addition, the hydroxyl groups adsorbed on the hydrated polymer produce a higher local pH, preventing dye molecules from protonation. On the other hand, when closer binding occurs by means of aromatic-aromatic interactions with polymers bearing charged aromatic groups such as PV10 and PK-Im, or by means of preferential solvation with amphiphilic polymers such as poly(vinyl pyrrolidone) [13], water from the hydration sphere of both interacting molecules is released, and protonation is also minimized. In the case of aromatic-aromatic interactions between charged aromatic groups, ion pairs may be formed through site-specific interactions that tend to confine in hydrophobic domains. These last terms explain the stabilization of the tetra-anionic form of TPPS in the presence of PK-Im at pH as low as 1.8.

All these facts have their correlate in the fluorescence behavior of the different systems, as can be seen in Fig. 4. Thus, the characteristic fluorescence band at 680 nm of the di-anionic species of TPPS is found in the presence of the three polymers. The characteristic bands at 642 and 706 nm of the tetra-anionic species of TPPS appeared shifted to lower energies up to 652 and 715 nm in the presence of PK-Im, corresponding to the shift on the absorbance band of the stabilized monomeric species. On the contrary, these bands do not appear in the presence of PV10, since H-aggregates do not fluoresce. Interestingly, only one band appears at 660 nm in the presence of CS when the molecule is excited at 414 nm, corresponding to the hydrated tetra-anionic monomer, which highlights that the interaction with the rigid, chiral polymer produces specific molecular and photophysical properties [43,44].

3.2. Colloidal suspensions

As a first step to fabricate the aerogels, colloidal suspensions have been produced. As stated in the experimental part, CS and ChS stock solutions are simultaneously dropped into an aqueous solution placed in a container with the aid of two syringes. In order to

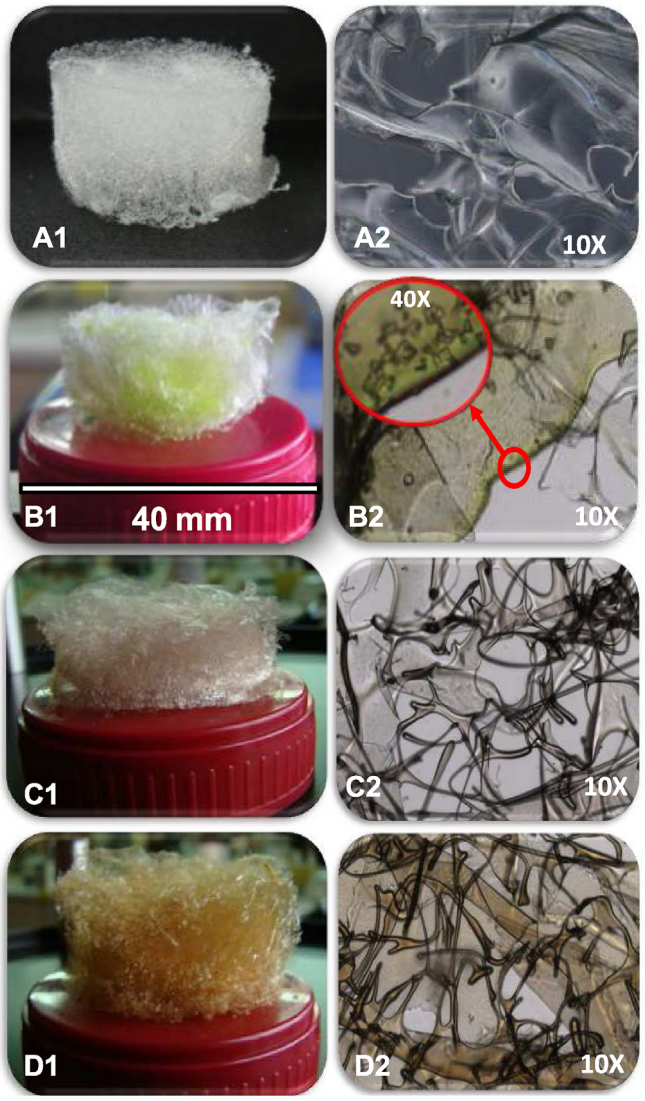

Fig. 7. Optical images without magnification (×1) and magnified 10-fold (×2) of aerogels made of CS/ChS (A1 and A2), CS/TPPS/ChS (B1 and B2), CS/TPPS/PV10/ChS (C1 and C2), and CS/TPPS/PK-Im/ChS (D1 and D2).

incorporate TPPS into the colloidal suspensions, TPPS/aromatic polymer complexes were placed in the receiving container. However, when placing pristine TPPS in the receiving container and further adding the polysaccharides, a green macroprecipitate was obtained. Colloidal suspensions were, then, effectively obtained in this case by adding TPPS to the syringe containing the also negatively charged ChS, and subtracting the amount of the dye from the amount of ChS, so that the total negative charges remain unchanged. The colloidal suspensions achieved were stable for at least 3 months, as can be seen in Figs. 5 and 6, where the apparent hydrodynamic diameters and zeta potentials of all the formulations have been plotted as a function of time. It can be seen that colloidal suspensions obtained in the absence of the dye or any of the aromatic polyelectrolytes presented an apparent particle size of around 320 nm, with PDI values ranging between 0.19 and 0.22. In addition, the zeta potential is positive and higher than 30 mV, which ensures the stability of the particles since particle aggregation is avoided by charge repulsion. The addition of TPPS, pristine or complexed with the aromatic polycations, produced an increase of the apparent size and of the zeta potential, without jeopardizing the stability. The quality of the colloidal suspensions, in addition to their stability, is also confirmed by the low PDI values found, which ranged between 0.20 and 0.25 for the formulations free of aromatic polycations, 0.20 and 0.22 for the formulations containing PV10, and 0.29 and 0.35 for the formulations containing PK-Im, indicating narrow monomodal distributions.

3.3. Aerogels

By freeze-drying the above mentioned colloidal suspensions, solids with different composition and macroscopic aspect arise, as can be seen in Fig. 7. The dimensions of the quasi cylindrical materials achieve around 30 mm of diameter and 15 mm of height. The porosity of the aerogels was higher than 99%, as theoretically calculated considering a density of the solid part of the materials higher than 0.779 g/cm^3. This threshold value was corroborated by immersion of the aerogels in cyclohexane. As can be also seen in Fig. 7, the aerogels are composed of microfibers and microsheets which correlate with other published aerogels made from polyelectrolyte nanocomplexes [45]. The aerogels containing TPPS and no aromatic polymeric species presented TPPS non-homogenously dispersed in the material. Optical microscopy reveals, in addition, the formation of dye crystals on the surface of the microsheets. This is due to that the interaction of the dye with CS is mainly ruled by long-range electrostatic interactions that are quenched by the negatively charged ChS. Thus, the tetra-anionic dye is released to the bulk, and, deprived from the stabilization produced by the polycation, protonates at the pH of the suspension. During freezing, the resulting di-anionic species migrate with the liquid water to the

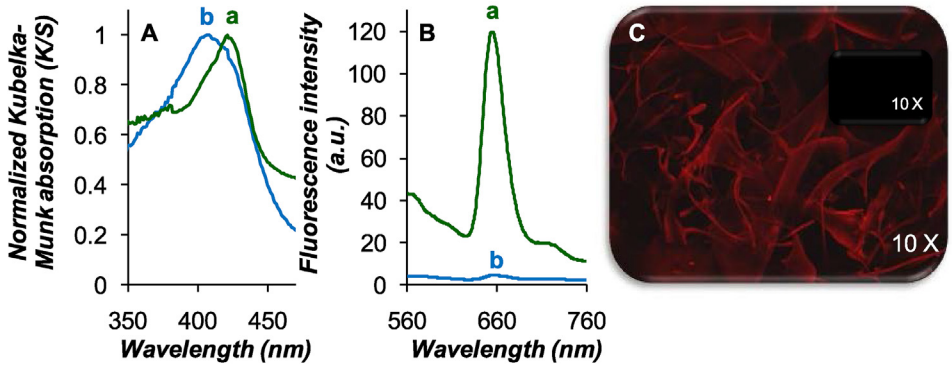

Fig. 8. A: Kubleka-Munk absorption spectra of CS/TPPS/PK-Im/ChS (a), and CS/TPPS/PV10/ChS (b); B: fluorescence spectra of solid aerogels made of CS/TPPS/PK-Im/ChS (a, excitation at 424 nm), and CS/TPPS/PV10/ChS (b, excitation at 400 nm); C: fluorescence confocal micrograph of solid aerogels made of CS/TPPS/PK-Im/ChS (main), and CS/TPPS/PV10/ChS (inset).

center of the solid, and J-aggregates of the dye crystallize or are deposited on the microsheets, furnishing the non-homogenous green color. On the contrary, aerogels containing PK-Im and PV10 presented homogenous coloration, indicating the homogenous dispersion of the dye on the entire material. Those containing PK-Im presented a brownish color, consistent with dispersed monomeric dye species, and those containing PV10 tend to be colorless consistent with the stacked dyes forming H-aggregates. The state of aggregation of TPPS complexed with aromatic polycations in the solids was confirmed by solid UV–vis diffuse reflectance and fluorescence spectroscopies (see Fig. 8). The Kubleka-Munk absorption shows absorption maxima at 407 and 421 nm for the dye in the solids containing PV10 and PK-Im, respectively, indicating that, after freeze-drying, the same state of aggregation of the dye is found both in the solid material and in solution in the presence of the respective aromatic polyelectrolytes. Emission spectra of the solid aerogels containing PK-Im show emission peaks centered at 652 and 715 nm when irradiated at 424 nm, coincident with the emission of the PK-Im/TPPS complex in solution. On the contrary, the aerogels containing PV10 did not show emission when irradiated at 400 nm, as neither did the PV10/TPPS complex in solution. The observation of the samples by confocal fluorescence microscopy correlates with the above statements, as can be seen in Fig. 8C, where microfibers and microsheets of the aerogels containing PK-Im show luminescent properties which are not observed for those containing PV10.

The aerogels presented here are fabricated by a simple, low-cost production protocol, avoiding chemical reactions producing new covalent bonds and the use of any organic solvent. The simplicity of the formulation versus the high performance in terms of the control of the state of aggregation and dispersibility of a photosensitizer such as TPPS is an advantage of these materials. The modulation of these properties of the photosensitizer is linked to the fundamental concept of aromatic-aromatic interactions between charged dyes and complementary charged aromatic polymers, so that, further projections are envisaged in a wide range of applications not only in medicine, but also in heterogeneous photocatalysis. Finally, the stability of these materials stored at room temperature in the dark has been corroborated by solid UV–vis quality control procedures after 112 days. This makes these materials easy to store and transport, conditions necessary for their adequate management.

4. Conclusions

The state of aggregation of TPPS and the transition pH between the di-anionic and the tetra-anionic species of the dye can be controlled in solution by means of aromatic polycations. Thus PK-Im stabilizes complexed monomeric tetra-anionic dye molecules up to pHs lower than 2.0, and PV10 stabilizes H-aggregates of the tetra-anionic species up to pH lower than 3.0. The state of aggregation and the photophysical properties associated can be transferred to solid materials composed of CS and ChS. Thus, aerogels made of the two polysaccharides, and containing TPPS/PK-Im and TPPS/PV10 complexes have been synthesized, showing a microstructure consisting of microfibers and microsheets, and porosity higher than 99%. The state of aggregation of the dye shown in solution has been conserved in the solids, so that H-aggregates have been found in the presence of PV10, whereas monomeric complexed dye molecules have been found in the presence of PK-Im. In addition, the respective complexes dispersed homogenously on the entire material. On the contrary, assays aiming at incorporating TPPS at pH 4.7 in the solid material resulted in non-homogenous distribution of J-aggregates and formation of microcrystals on the microsheets. This study highlights the potential of aromatic-aromatic interactions to achieve 1) control of the state of aggregation of dyes in solution, 2) control of the state of aggregation of dyes in the solid state, 3) control of the dispersion of the dyes in solid materials. These findings, both in solution and in the solid state, promote significant improvements for the use of dyes whose control of aggregation and dispersion in the final material is critical.

Acknowledgment

The authors thank Fondecyt Regular (Grants No 1120514, 1150899, and 1161450, Chile), FIC-R Los Ríos 2011 (Chile) and Waseda Advanced Research Institute for Science & Engineering (Grant No. 24225003, MEXT Japan).

References

[1] Martín-Gomisa L, Barea EM, Fernández-Lázaroa F, Bisquert J, Sastre-Santos Á. Dye sensitized solar cells using non-aggregated silicon phthalocyanines. J Porphyr Phthalocyanines 2011;15(09n10):1004–10.
[2] Tardivo JP, Del Giglio A, de Oliveira CS, Gabrielli DS, Junqueira HC, Tada DB, et al. Methylene blue in photodynamic therapy: from basic mechanisms to clinical applications. Photodiagn Photodyn Ther 2005;2(3):175–91.
[3] Mulhern KR, Detty MR, Watson DF. Aggregation-Induced increase of the quantum yield of electron injection from chalcogenorhodamine dyes to TiO_2. J Phys Chem C 2011;115(13):6010–8.
[4] Tsuchikawa R, Ahn HY, Yao S, Belfield KD, Ishigami M. Photosensitization of carbon nanotubes using dye aggregates. J Phys Condens Matter 2011;23(20):202204.
[5] Bonnett R. Photosensitizers of the porphyrin and phthalocyanine series for photodynamic therapy. Chem Soc Rev 1995;24(1):19–33.
[6] Dolmans DEJGJ, Fukumura D, Jain RK. Photodynamic therapy for cancer. Nat Rev Cancer 2003;3(5):380–7.
[7] Niedre MJ, Yu CS, Patterson MS, Wilson BC. Singlet oxygen luminescence as an in vivo photodynamic therapy dose metric: validation in normal mouse skin with topical amino-levulinic acid. Br J Cancer 2005;92(2):298–304.
[8] Weishaupt KR, Gomer CJ, Dougherty TJ. Identification of singlet oxygen as the cytotoxic agent in photo-inactivation of a murine tumor. Cancer Res 1976;36(7 Part 1):2326–9.
[9] Maiti NC, Mazumdar S, Periasamy N. J- and H-aggregates of porphyrin–surfactant complexes: time-resolved fluorescence and other spectroscopic studies†. J Phys Chem B 1998;102(9):1528–38.
[10] Moreno-Villoslada I, Murakami T, Nishide H. Comment on "J- and H-aggregates of 5,10,15,20-Tetrakis-(4–sulfonatophenyl)-porphyrin and interconversion in PEG-b-P4VP micelles". Biomacromolecules 2009;10(12):3341–2.
[11] Zhao L, Ma R, Li J, Li Y, An Y, Shi L. Reply to comment on "J- and H-aggregates of 5,10,15,20-Tetrakis-(4-sulfonatophenyl)-porphyrin and interconversion in PEG-b-P4VP micelles". Biomacromolecules 2009;10(12):3343–4.
[12] Toncelli C, Pino-Pinto JP, Sano N, Picchioni F, Broekhuis AA, Nishide H, et al. Controlling the aggregation of 5,10,15,20-tetrakis-(4-sulfonatophenyl)-porphyrin by the use of polycations derived from polyketones bearing charged aromatic groups. Dyes Pigments 2013;98(1):51–63.
[13] Gómez-Tardajos M, Pino-Pinto JP, Díaz-Soto C, Flores ME, Gallardo A, Elvira C, et al. Confinement of 5,10,15,20-tetrakis-(4-sulfonatophenyl)-porphyrin in novel poly(vinylpyrrolidone)s modified with aromatic amines. Dyes Pigments 2013;99(3):759–70.
[14] Egawa Y, Hayashida R, Anzai J-i. pH-Induced interconversion between J-aggregates and H-aggregates of 5,10,15,20-tetrakis(4-sulfonatophenyl) porphyrin in polyelectrolyte multilayer films. Langmuir 2007;23(26):13146–50.
[15] Synytsya A, Blafkova P, Ederova J, Spevacek J, Slepicka P, Kral V, et al. pH-controlled self-assembling of meso-tetrakis(4-sulfonatophenyl)porphyrin-chitosan complexes. Biomacromolecules 2009;10(5):1067–76.
[16] Zhang L, Lu Q, Liu M. Fabrication of chiral langmuir–schaefer films from achiral TPPS and amphiphiles through the adsorption at the air/water interface. J Phys Chem B 2003;107(11):2565–9.
[17] Wu J-J, Li N, Li K-A, Liu F. J-aggregates of diprotonated tetrakis(4-sulfonatophenyl)porphyrin induced by ionic liquid 1-butyl-3-methylimidazolium tetrafluoroborate. J Phys Chem B 2008;112(27):8134–8.
[18] Soedjak HS. Colorimetric determination of carrageenans and other anionic hydrocolloids with methylene blue. Anal Chem 1994;66(24):4514–8.
[19] Moreno-Villoslada I, Torres C, González F, Shibue T, Nishide H. Binding of methylene blue to polyelectrolytes containing sulfonate groups. Macromol Chem Phys 2009;210(13–14):1167–75.
[20] Moreno-Villoslada I, González F, Arias L, Villatoro JM, Ugarte R, Hess S, et al. Control of C.I. basic violet 10 aggregation in aqueous solution by the use of poly(sodium 4-styrenesulfonate). Dyes Pigments 2009;82(3):401–8.
[21] López Arbeloa I, Ruiz Ojeda P. Dimeric states of rhodamine B. Chem Phys Lett 1982;87(6):556–60.
[22] Moreno-Villoslada I, Fuenzalida JP, Tripailaf G, Araya-Hermosilla R, Pizarro GdC, Marambio OG, et al. Comparative study of the self-aggregation of

rhodamine 6G in the presence of poly(sodium 4-styrenesulfonate), poly(N-phenylmaleimide-co-acrylic acid), poly(styrene-alt-maleic acid), and poly(-sodium acrylate). J Phys Chem B 2010;114(37):11983–92.
[23] Martínez Martínez V, López Arbeloa F, Bañuelos Prieto J, López Arbeloa I. Characterization of rhodamine 6G aggregates intercalated in solid thin films of laponite clay. 2 fluorescence spectroscopy. J Phys Chem B 2005;109(15):7443–50.
[24] Schwarz G. Cooperative binding to linear biopolymers. Eur J Biochem 1970;12(3):442–53.
[25] Gradova MA, Lobanov AV. Photophysical properties and aggregation behavior of transition metal tetraphenylporphyrin tetrasulfonate complexes in microheterogeneous media. Macroheterocycles 2013;6(4):340–4.
[26] Gröhn F. Electrostatic self-assembly as route to supramolecular structures. Macromol Chem Phys 2008;209(22):2295–301.
[27] Ruthard C, Schmidt M, Gröhn F. Porphyrin–polymer networks, worms, and nanorods: pH-triggerable hierarchical self-assembly. Macromol Rapid Commun 2011;32(9–10):706–11.
[28] Willerich I, Schindler T, Ritter H, Grohn F. Controlling the size of electrostatically self-assembled nanoparticles with cyclodextrin as external trigger. Soft Matter 2011;7(11):5444–50.
[29] Willerich I, Gröhn F. Molecular structure encodes nanoscale assemblies: understanding driving forces in electrostatic self-assembly. J Am Chem Soc 2011;133(50):20341–56.
[30] Faul CFJ, Antonietti M. Ionic self-assembly: facile synthesis of supramolecular materials. Adv Mater 2003;15(9):673–83.
[31] Decher G. Fuzzy nanoassemblies: toward layered polymeric multicomposites. Science 1997;277(5330):1232–7.
[32] Zhao Y, Tanaka M, Kinoshita T, Higuchi M, Tan T. Controlled release and entrapment of enantiomers in self-assembling scaffolds composed of β-sheet peptides. Biomacromolecules 2009;10(12):3266–72.
[33] Park M-K, Onishi K, Locklin J, Caruso F, Advincula RC. Self-assembly and characterization of polyaniline and sulfonated polystyrene multilayer-coated colloidal particles and hollow shells. Langmuir 2003;19(20):8550–4.
[34] Villari V, Mineo P, Scamporrino E, Micali N. Role of the hydrogen-bond in porphyrin J-aggregates. RSC Adv 2012;2(33):12989–98.
[35] Uemori Y, Takinami S, Takahashi A, Munakata H, Imai H, Nakagawa S, et al. Effect of aromatic-aromatic interaction on ligand binding to zinc porphyrins. Inorg Chim Acta 1994;224(1):157–61.
[36] Stojanović SĐ, Medaković VB, Predović G, Beljanski M, Zarić SD. XH/π interactions with the π system of porphyrin ring in porphyrin-containing proteins. JBIC J Biol Inorg Chem 2007;12(7):1063–71.
[37] Moreno-Villoslada I, Torres-Gallegos C, Araya-Hermosilla R, Fuenzalida JP, Marambio OG, Pizarro GdC, et al. Different models on binding of aromatic counterions to polyelectrolytes. Mol Cryst Liq Cryst 2010;522(1). 136/[436]-147/[447].
[38] Moreno-Villoslada I, Torres-Gallegos Cs, Araya-Hermosilla R, Nishide H. Influence of the linear aromatic density on methylene blue aggregation around polyanions containing sulfonate groups. J Phys Chem B 2010;114(12):4151–8.
[39] Flores ME, Sano N, Araya-Hermosilla R, Shibue T, Olea AF, Nishide H, et al. Self-association of 5,10,15,20-tetrakis-(4-sulfonatophenyl)-porphyrin tuned by poly(decylviologen) and sulfobutylether-β-cyclodextrin. Dyes Pigments 2015;112:262–73.
[40] Vidal A, Giacaman A, Oyarzun-Ampuero FA, Orellana S, Aburto I, Pavicic MF, et al. Therapeutic potential of a low-cost device for wound healing: a study of three cases of healing after lower-extremity amputation in patients with diabetes. Am J Ther 2013;20(4):394–8.
[41] Franca EF, Lins RD, Freitas LCG, Straatsma TP. Characterization of chitin and chitosan molecular structure in aqueous solution. J Chem Theory Comput 2008;4(12):2141–9.
[42] Synytsya A, Synytsya A, Blafkova P, Volka K, Král V. Interaction of meso-tetrakis(4-sulphonatophenyl)porphine with chitosan in aqueous solutions. Spectrochim Acta Part A Mol Biomol Spectrosc 2007;66(2):225–35.
[43] Polo CF, Frisardi AL, Resnik ER, Schoua AE, Batlle AM. Factors influencing fluorescence spectra of free porphyrins. Clin Chem 1988;34(4):757–60.
[44] Seybold PG, Gouterman M. Porphyrins. J Mol Spectrosc 1969;31(1):1–13.
[45] Sanhueza L, Castro J, Urzúa E, Barrientos L, Oyarzun-Ampuero F, Pesenti H, et al. Photochromic solid materials based on poly(decylviologen) complexed with alginate and poly(sodium 4-styrenesulfonate). J Phys Chem B 2015;119(41):13208–17.